Scientia Iranica B (2021) 28(1), 355–370

SCIENTIA IRANICA

Sharif University of Technology
Scientia Iranica
Transactions B: Mechanical Engineering
http://scientiairanica.sharif.edu

Research Note

Design, modeling, and impedance control of a new in-pipe inspection robot equipped by a manipulator

H. Tourajizadeh*, **V. Boomeri**, **S. Afshari**, **and M. Azimi**

Department of Mechanical Engineering, Faculty of Engineering, Kharazmi University, Tehran, P.O. Box 3197937551, Iran.

Received 1 April 2019; received in revised form 4 July 2019; accepted 7 September 2019

KEYWORDS
Robot design and modeling;
In-pipe inspection robots;
Wheeled wall-pressed robot;
Manipulator;
Impedance control.

Abstract. In this paper, a new in-pipe robot is designed and modeled, which is equipped by a manipulator in order to perform repairing tasks within the pipelines. Also, in order to provide a good manipulation process, impedance control is designed and implemented for the robot. Most of the in-pipe robots are limited to performing inspection operations and are not capable of conducting manipulation tasks. In order to cover the mentioned deficiency, the robot is redesigned by adding a manipulator to the main body of the moving platform. Afterwards, the model of the overall robot is extracted. Finally, impedance control is also designed and implemented for the robot so that, not only can the position of the end-effector be controlled, but also the required force to cover the repairing task can be precisely provided. The correctness of modeling and efficiency of the proposed mobile in-pipe robot is verified by conducting some simulation scenarios in MATLAB. It will be seen that with the aid of the proposed mechanism and employing the designed force controlling strategy, the manipulation process of the robot in the pipes can be realized successfully.

1. Introduction

There are several milliard kilometer pipelines (with different functionality including water pipeline, oil pipeline, etc.) which need to be completely inspected about every seven years. For many of the mentioned pipelines, human entry is not possible as a result of the pipeline diameter, environmental conditions, and flowing fluids, etc., which highlights the effective role of robots to cover the inspection processes. In-pipe inspection robots are widely applicable nowadays in order to inspect pipes not usually reachable by humans. It is unavoidable that all kinds of pipeline are damageable and need periodic inspection as a result of chemical interaction between the pipe walls and the flowing fluids. Also, there are numerous sources of fluidic resistance, including external obstacles, corrosion, etc. which can malfunction in the path of the fluid flow, gas and other pipe lines that are filled with dangerous fluids harmful to humans. Water pipelines which commonly have a small diameter and are impassable by humans are the main examples of these pipes. Different kinds of mechanisms are proposed, each of which solves the special challenge of in-pipe inspections robots. Inspection without the possibility of manipulating the operation is not efficient. Also, it is obvious that improving the structure of the robot and designing a proper controller are significant when wishing to perform inspection and manipulation processes simultaneously. The first generation of inspection robots was based on mobile robots. Much research has been devoted to modeling

*. *Corresponding author.*
E-mail address: Tourajizadeh@khu.ac.ir (H. Tourajizadeh)

doi: 10.24200/sci.2020.53117.3068

and analyzing different kinds of mobile robot so far. Mobile robots are widely used as inspectors and thus are extremely studied by many researchers. Thanjavur and Rajagopalan modeled the dynamics of Wheeled Mobile Robots (WMRs) using Kane's approach for non-holonomic systems. Since the Kane's approach provides a systematic modelling scheme, the method proposed in this paper can be easily generalized to any model of WMRs with various wheel types and configurations and for any loading conditions [1]. Also, the same procedure is used in [2] for a wheeled mobile manipulator system using Kane's dynamic equations, in which both non-holonomic constraints associated with slipping and skidding are included, as well as constraint related to tip over avoidance. In order to avoid the Lagrangian formulation which is a time-consuming process in dynamic modeling, the mathematical modeling of a robotic system composed of n flexible links and a mobile platform has been considered in [3] using Gibbs-Appell formulation. In this regard, Korayem and Dehkordi investigated the dynamic equations of an n-flexible link manipulator with revolute-prismatic joints. The effects of manipulator locomotion by the mobile platform with non-holonomic kinematic constraints are considered in [4], which cause serious motion limitations in addition to creating special dynamic interaction between the manipulator and platform. The mentioned formulation approach has also been applied for dynamic modeling of non-holonomic wheeled mobile robotic manipulators, which consist of a serial manipulator with elastic joints and an autonomous wheeled mobile platform. The approach of Gibbs-Appell (G-A) formulation in recursive form is employed here to avoid the computation of Lagrange multipliers associated with the non-holonomic constraints [5]. Mobile robots can also be combined with other robotic systems such as cable robots. Therefore, using the mentioned Gibbs-Appell method in [6], the authors have extracted the dynamic modeling and control of a mobile cable-suspended parallel robot with a wheeled mobile platform, considering the weight of the cable. In a general approach, a symbolic algorithm is proposed by Korayem and Shafei capable of deriving the equations of motion of n-rigid link manipulators with Revolute-Prismatic (R-P) joints which are mounted on a mobile platform [7]. The Gibbs-Appell method has also been used to present a new formulation in order to solve a large group of high order non-holonomic constrained systems without using Lagrange multipliers [8].

However, for our case study which is in pipe inspection, the mentioned mobile robots need to be improved in such a way that they can be adjusted with in-pipe environments. The most applicable types of the mentioned robots are: wheeled, caterpillar, snake, legged, inchworm, screw, and PIG. The most successful mechanisms by which the highest maneuverability can be provided are wall-pressed types known as "hybrid locomotion". In this type, the wall not only tolerates the weight of the robot but also provides an additional force to create the stability of the robot. Additionally, the required friction of the robot propulsion can be prepared by the aid of the wall. This type of robot can be itself divided into a caterpillar wall-pressed type, wheeled wall-pressed type, and wheeled wall pressing screw type depending on its locomotion mechanism [9]. Fukuda et al. have developed an inchworm-type in-pipe inspection robot [10] while Roman et al. proposed the caterpillar type of this robot [11]. Since the wall-pressed type provides better stability for these kinds of robots, Iwashina et al. have developed a wall-pressed mechanism of in-pipe inspection robots which was able to navigate through inclined pipelines [12]. In these researches, the robot is not able to pass through the pipes with un-uniform geometrical cross sections since the leg lengths are not independently variable. Considering other research in this field, Li et al. have designed a novel active screw-driven in-pipe robot to inspect the condition of the pipeline. Since the wheels have rolling and steering motions, the robot has translational and rotational movements as a result of its screw motion, with respect to the axis of the pipe due to different values of the wheel steering angle. The robot can also overcome obstacles using the screw motion mode and the compensation of its suspension mechanism. Due to the special moving principle, the robot can also adapt circular and square tubes without any change of the structure [13]. In another paper by Ciszewski et al., a tracking inspection mobile robot with an active adaptation system is presented. It can be used for visual inspection of various pipelines. Mathematical modeling of the adaptation mechanisms that allow adjustment of the robot to different shapes and sizes of pipe is described considering the forward and inverse kinematics of the system. Simulation studies of robot motion, conducted in V-REP and MATLAB software are performed for horizontal and rough surfaces and horizontal pipe segments with connections and reducers [14]. Nayak and Pradhan presented corresponding investigations to design in-pipe robots considering their mobility, steerability, turning radius, size, shape, and online adaptability, flexibility, stability, control system, etc. and proposed a new model of an in-pipe inspection robot to overcome some critical design issues. This proposed model is a screw-drive type and wall-pressed adaptable wheeled in-pipe inspection robot. It is able to move through vertical and horizontal pipes, and it can easily pass through elbow connections of a pipe line [15]. Chang et al. presented a pipeline inspection robot with a linkage mechanical clutch, which consists of a novel belt driven with a ridged cone-shaped skate model that can be used to overcome irregular environmental barriers. The robot can be operated in various configurations and sizes of pipeline and can utilize the belt driven with a corrugate-ridged cone-shaped skate model to advance irregular barriers of a pipeline [16]. In another research by Ciszewski et al., modeling and simulation of a tracked mobile robot for pipe inspection are considered. The mechanical structure of the robot is described with a focus on pedipulators, used to change the pose of tracking drive modules to adapt to different pipe sizes and shapes [17]. Also, a simple design of these robots has been undertaken by Gargade and Ohol in a related paper, in which several experiments are conducted for pipes with different diameters, and the effectiveness of its steering mechanism is verified. This robot can be used for offline visual inspection of different pipe elements such as straight pipes, elbows, and reducers. Also, it can be used to locate the position of defects in the pipes [18].

Some research has been done in order to define the different locomotion mechanisms of in-pipe inspection robots. Guidelines have been built for a decision-making tool to help developers define needs and requirements when designing drive mechanisms for distinctive requisitions that fulfill predefined requirements and specifications of robotic development [19]. This work takes a novel approach of the guideline formation of Pipeline Robotics in order to reduce the costs of robotics. In [20], Kwon and Yi have presented the closed-form kinematic model of the pipeline inspection robot driven by three caterpillar wheel chains. Chablat et al. got the results from a multi-objective optimization process and used them to set the geometric and kinematic parameters of an in-pipe robot mechanism taking into account the environmental and design constraints [21]. The dynamic behavior of a sensor-based platform that travels through an underground pipeline network has been investigated by Gravalos et al. [22]. An in-pipe robot with active pipe-diameter adaptability and automatic adjusting tractive force was developed by Zhang and Yan, which is for long-distance inspection of main gas pipelines with different diameter series [23].

However, the literature is still poor regarding the controlling of in-pipe inspection robots. Kwon et al. used the position/force control of the wheels in order to control a mobile robot [24]. Zhang and Chen have used a fuzzy controller in order to control an in-pipe inspection robot [25]. Also, Gregory et al. planned the optimal path of a mobile manipulator with holonomic constraint employing an optimal control method [26]. However, in these researches, the force control of an in-pipe inspection robot equipped by a manipulator with variable legs is ignored, which could be significantly important in order to design an in-pipe robot that is supposed to move through damaged pipes. Although the force control of the manipulator of an in-pipe robot has not been studied so far, this controlling strategy has been applied to similar mobile robots or manipulators. In [27], a neuro-adaptive controller is proposed for simultaneous controlling of the position and force of a mobile manipulator in the presence of parametric uncertainties and unknown constraints. Carelli and Kelly have proposed an adaptive control for constraint robots in the presence of parametric uncertainties. The method consists of a Computed Torque Method (CTM) controller together with a compensator to neutralize the effect of uncertainties [28]. Another study is the design of an adaptive sliding mode controller through which the error of both position and force decreases exponentially [29]. Doulgeri and Arimoto have solved the problem of setting the position and force of the end-effector of a robot during its interaction with rigid surfaces by calculating the controlling input as a nonlinear function of position and force errors. This study, again, is in the presence of kinematic and kinetic uncertainties [30]. Similar research has been conducted in [31] considering the stability of the system.

Finally, a summary of different types of in-pipe robot is given in Table 1, which shows the different capabilities of the mentioned systems. The main topics which have been ignored in these researches can be mentioned as follows: Firstly, the proposed robots are not able to pass through pipes with different diameters or different geometrical shapes with any curvature profiles. Secondly, they are only equipped with inspector sensors and are not capable of manipulation operations. Based on the mentioned items, in this paper, a new mechanism is proposed, in which an additional module is added as the manipulator, whose legs are also adjustable to the diameter and geometrical shape of the pipes. Also, corresponding kinetic and kinematic modeling are developed by which the movement of the robot can be controlled.

Therefore, the proper mechanism of the in-pipe robot equipped by a manipulator is designed, which has adjustable leg length, and its related kinematics are developed. Afterward, the kinetics formulation of the robot is derived using the Lagrange method. In order to control the movement of the robot, a CTM is employed to provide acceptable maneuverability for the robot while impedance control is designed and applied to the robot to control the manipulation process. All of the modeling and controlling procedures are simulated in MATLAB to confirm the correctness and efficiency of the proposed robot. The results show that the proposed robot can not only inspect pipes with different diameters and geometrical shapes but can also successfully perform operational tasks to improve the inspected problems. The second section is related to design and extract the kinematic and kinetic modeling of the proposed in-pipe robot, which

Table 1. Comparison of different types of in-pipe inspection robot [15].

	Wheel type robot			Caterpillar type robot		Without wheel type robot		
Performance indicator	**Wheel type robot (simple structure)**	**Wheel type (wall-pressed type)**	**Screw-drive type robot**	**Caterpillar robot (simple structure type)**	**Caterpillar robot (wall-pressed type)**	**Leg type robot**	**Inchworm type robot**	**Snake type robot**
Vertical mobility	Poor	Very good	Very good	Fair	Very good	Very good	Fair	Fair
Steerability	Very good	Fair	Fair	Fair	Fair	Very good	Fair	Fair
Size and shape adaptability	Poor	Very good	Fair	Poor	Very good	Very good	Fair	Very good
Flexibility of robot	Rigid	Rigid	Less flexible	Rigid	Rigid	Rigid	Flexible	Flexible
Stability of robot	Poor	Very good	Very good	Fair	Fair	Fair	Fair	Fair
Motion efficiency	Fair	Fair	Very good	Fair	Very good	Very good	Very good	Fair
Number of actuators	Fair	Fair	Less	Less	Less	More	More	More
Wireless control	Fair	Very good	Fair	Fair	Fair	Poor	Poor	Poor

is equipped by a manipulator. Afterwards, in section three, the required controlling strategies which are proposed for the locomotion and manipulation process of the robot are presented according to the CTM and impedance control, respectively. In section four, the correctness and efficiency of the proposed mobile robot, its installed manipulator and the corresponding controllers are investigated with the aid of some simulation studies performed in MATLAB. The last section is devoted to conclusions and discussions. It is shown that the proposed integration of a mobile inspection robot together with a manipulator, can successfully manage inspection processes in pipes with different diameters, while any required manipulation can also be implemented simultaneously.

2. Design and modeling

The robot is a kind of wall-pressed wheeled in-pipe robot and is designed in a way that can move through pipeline with different diameters or geometrical cross-sections at high speed.

To cover the mentioned requirements, three prismatic legs equipped with a suspension system is designed, through which three wheels are installed and fixed to the inside wall of the pipes. Then, a 3-DOF manipulator is mounted on its centroid to prepare the robot for manipulating and operational tasks. A simple schematic of the proposed in-pipe robot can be seen in Figure 1. In this design, the angle between the legs is 120 degrees, the robot motion is straightforward along the pipe, and so the robot has no rotation about the pipe direction. In the kinematics section, it is desired to extract the relation between the end-effector motion and wheel rotation. To do so, D-H transformation

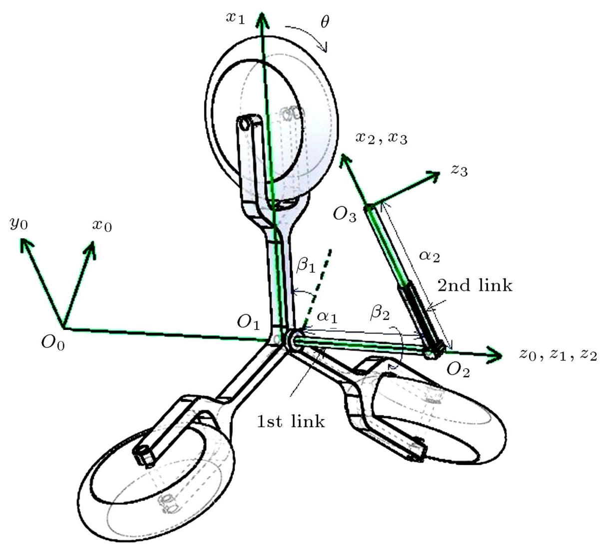

Figure 1. The designed in-pipe robot with a manipulator.

Table 2. D-H table of the designed in-pipe robot.

Link no.	a_i	α_i	d_i	θ_i
1	0	0	$r\theta$	β_1
2	0	0	a_1	β_2
3	a_2	0	0	0

matrices are employed [32]. The coordinates, according to D-H, are attached to the manipulator of the robot, as Figure 1. Here, the initial angle of the robot about the pipeline axis is shown by β_1. Thus, the related D-H parameters can be established as Table 2.

The coordinates of the end-effector, with respect to the coordinates attached to the second link, are shown by $p_3 = \begin{bmatrix} 0 & 0 & 0 & 1 \end{bmatrix}^T$, then we have:

$$p_{3\_0} = A_1 A_2 A_3 p_3 = A_{3\_0} p_3 = \begin{bmatrix} x \\ y \\ z \\ 1 \end{bmatrix} = \begin{bmatrix} a_2 C_{\beta_1+\beta_2} \\ a_2 S_{\beta_1+\beta_2} \\ r\theta + a_1 \\ 1 \end{bmatrix}. \tag{1}$$

Eq. (1) expresses the location of the end-effector according to the reference coordinate. Considering $q = \begin{bmatrix} \theta & \beta_2 & a_2 \end{bmatrix}^T$ as the generalized coordinate of the system, the speed kinematics can be extracted using the Jacobian matrix:

$$J = \frac{\partial p_{3\_0}}{\partial q} = \begin{bmatrix} 0 & -a_2 S_{\beta_1+\beta_2} & C_{\beta_1+\beta_2} \\ 0 & a_2 C_{\beta_1+\beta_2} & S_{\beta_1+\beta_2} \\ r & 0 & 0 \end{bmatrix}. \tag{2}$$

And, finally, the speed relation between the workspace and joint space can be introduced as:

$$\dot{p}_{3\_0} = J\dot{q} = \begin{bmatrix} \dot{a}_2 C_{\beta_1+\beta_2} - a_2\dot{\beta}_2 S_{\beta_1+\beta_2} \\ \dot{a}_2 S_{\beta_1+\beta_2} + a_2\dot{\beta}_2 C_{\beta_1+\beta_2} \\ r\dot{\theta} \end{bmatrix}. \tag{3}$$

Notice that the proposed in-pipe robot in this paper is limited to movement through a pipe with a predefined curve, and thus its global rotational position is a function of its translational position and is not an independent Degrees Of Freedom (DOF). Thus, the angle of the robot, which is the same as the angle of the pipe, is not an independent DOF. Consequently, the non-holonomic constraint of mobile robots will be converted to a holonomic one, which represents the relation between the translational movement of the robot across the pipe with the rotational angle of the wheels. This constraint is presented at the third row of the Jacobian matrix and is satisfied accordingly. In order to extract the inverse position kinematics of the system, it is required to solve a set of simultaneous equations with three equations and three unknowns as follows:

$$q = \begin{bmatrix} \theta \\ \beta_2 \\ a_2 \end{bmatrix} = \begin{bmatrix} (z - a_1)/r \\ \operatorname{atan2}(y, x) - \beta_1 \\ \sqrt{x^2 + y^2} \end{bmatrix}. \tag{4}$$

Again, here, it is possible to introduce the inverse speed kinematics using the inverse of the extracted Jacobian matrix.

Employing the Lagrange method, the potential and kinetic energy of the robot are extracted here, and the dynamics equations are obtained. First, the kinetic energy of the system is calculated. The kinetic energy can be calculated as follows:

$$\begin{aligned} K_e =& K_1 + K_2 + K_3 + K_4 + K_5 + K_6 \\ =& \frac{1}{2} r^2 \dot{\theta}^2 (m_{a_1} + m_{a_2} + m_b + 3m_w) + \frac{3}{4} m_w r^2 \dot{\theta}^2 \\ &+ \frac{1}{2} m_{a_2} \dot{a}_2^2 + \frac{1}{6} m_{a_2} a_2^2 \dot{\beta}_2^2 + \frac{1}{4} m_{a_1} r_{a_1}^2 \dot{\beta}_2^2, \end{aligned}$$

$$K_1 = 0.5(m_{a1} + m_{a2} + m_b + 3m_w)(r\dot{\theta})^2,$$

$$K_2 = 3(0.5 I_w \dot{\theta}^2), \qquad K_3 = 0.5 m_{a_2} \dot{a}_2^2,$$

$$K_4 = 0.5 m_{a_2} (0.5 a_2 \dot{\beta}_2)^2, \qquad K_5 = 0.5 I_{a_2} \dot{\beta}_2^2,$$

$$K_6 = 0.5 I_{a_1} \dot{\beta}_2^2, \tag{5}$$

where I_w is the inertia momentum of each wheel, I_{a_1} is the momentum inertia of the first link and I_{a_2} is the momentum inertia of the second link. For each case, the momentums are about the axis of each part and, for the second link, it is about the axis perpendicular to the link around the centroid of the link. Also, m_w is the mass of the wheels, m_{a_1} is the mass of the first link and m_{a_2} is the mass of the second link. Moreover, r_{a_1} is the radius of the first link, m_t is the total mass of the robot, K_1 is the translational kinetic energy of the robot, K_2 is the rotational kinetic energy of the wheels, K_3 is the translational kinetic energy of the second prismatic link, K_4 is the translational kinetic energy of the centroid of the second link, K_5 is the rotational kinetic energy of the second link, K_6 is the rotational kinetic energy of the first link about its axis and K_e is the total kinetic energy of the system.

In order to calculate the potential energy, the axis of the pipe is considered as the potential origin of the system. Thus, the only part of the robot which has potential energy is the second link of the robot where its Y component, with respect to the reference coordinate, represents the height of the link and which can be calculated by multiplication of the transformation matrix by its coordinates, with respect to its local axis:

$$M(q)=\begin{bmatrix}\frac{1}{2}r^2(2m_{a_1}+2m_{a_2}+2m_b+9m_w) & 0 & 0\\ 0 & \frac{1}{3}m_{a_2}a_2^2+\frac{1}{2}m_{a_1}r_{a_1}^2 & 0\\ 0 & 0 & m_{a_2}\end{bmatrix},$$

$$CG\,(q,\dot{q})=\begin{bmatrix}0\\ \\ \frac{1}{2}m_{a_2}ga_2C_{\beta_1+\beta_2}\\ \\ \frac{1}{2}m_{a_2}gS_{\beta_1+\beta_2}-\frac{1}{3}a_2\dot{\beta}_2^2\end{bmatrix}. \tag{10}$$

Box I

$$Cm_{a_2}=\begin{bmatrix}Xm_{a_2}\\ Ym_{a_2}\\ Zm_{a_2}\\ 1\end{bmatrix}=A_{2_0}([0.5,1,1,1]p_2),$$

$$Pe=m_{a_2}gh_{a_2}=0.5m_{a_2}ga_2S_{\beta_1+\beta_2},$$

$$Ym_{a_2}=h_{a_2}=0.5a_2S_{\beta_1+\beta_2}, \tag{6}$$

where, g is the gravitational acceleration. We can now write the Lagrange function as follows:

$$\begin{aligned}La=&K_e-Pe=\frac{1}{6}m_{a_2}a_2^2\dot{\beta}_2^2+\frac{1}{2}m_{a_2}\dot{a}_2^2\\ &+\frac{1}{4}m_{a_1}r_{a_1}^2\dot{\beta}_2^2+\frac{1}{2}r^2\dot{\theta}^2(m_{a_1}+m_{a_2}+m_b+3m_w)\\ &+\frac{3}{4}m_wr^2\dot{\theta}^2-\frac{1}{2}m_{a_2}ga_2S_{\beta_1+\beta_2}.\end{aligned} \tag{7}$$

For extracting the dynamic equations, we have:

$$\tau_i-3F_S.r=\frac{d}{dt}\left(\frac{\partial La}{\partial\dot{q}_i}\right)-\left(\frac{\partial La}{\partial q_i}\right),$$

$$\tau=\begin{bmatrix}\tau_1\\ \tau_2\\ \tau_3\end{bmatrix}=\begin{bmatrix}\tau_\theta\\ \tau_{\beta_2}\\ f_{a_2}\end{bmatrix}$$

$$=\begin{bmatrix}\frac{1}{2}r^2\ddot{\theta}(2m_{a_1}2m_{a_2}+2m_b+9m_w)+3rF_S\\ \\ \ddot{\beta}_2\left(\frac{1}{3}m_{a_2}a_2^2+\frac{1}{2}m_{a_1}r_{a_1}^2\right)+\frac{1}{2}m_{a_2}ga_2C_{\beta_1+\beta_2}\\ \\ \frac{1}{6}m_{a_2}\left(-2a_2\dot{\beta}_2^2+6\ddot{a}_2+3gS_{\beta_1+\beta_2}\right)\end{bmatrix}, \tag{8}$$

where F_s is the friction force between each wheel and pipe surface, τ_θ is the torque of the wheels, τ_{β_2} is the torque of the first link and f_{a_2} is the prismatic force of the second link. Considering Eq. (8), it is possible to control robot movement using the CTM strategy. The direct dynamics of the system are now solved as the plant of the robot in order to verify the calculated inverse dynamics. To do so, the dynamic equation of the system is first rewritten in the following matrix form:

$$\tau=M(q)\ddot{q}+CG\,(q,\dot{q})+\begin{bmatrix}3rF_S\\ 0\\ 0\end{bmatrix}. \tag{9}$$

Thus, the inertia matrix M and centrifugal/Coriolis matrix, CG, will be obtained by Eq. (10) as shown in Box I.

Considering the two mentioned matrices and the torque of the motors as the plant input, the actual acceleration vector of the generalized coordinate can be calculated. It is possible to calculate the response of the generalized coordinates by solving the following set of simultaneous coupled differential equations:

$$\ddot{q}=\begin{bmatrix}\ddot{\theta}\\ \ddot{\beta}_2\\ \ddot{a}_2\end{bmatrix}=M^{-1}(\tau-CG)$$

$$=\begin{bmatrix}2\tau_1/r^2(2m_{a_1}+2m_{a_2}+2m_b+9m_w)\\ \\ \frac{6\left(\tau_2-\frac{1}{2}m_{a_2}ga_2C_{\beta_1+\beta_2}\right)}{(2m_{a_2}a_2^2+3m_{a_1}r_{a_1}^2)}\\ \\ \frac{1}{m_{a_2}}\left(\tau_3-\frac{1}{6}m_{a_2}\left(-2a_2\dot{\beta}_2^2+3gS_{\beta_1+\beta_2}\right)\right)\end{bmatrix}. \tag{11}$$

With the aid of the mentioned calculated vector of the joints' acceleration, it is possible to calculate their response in MATLAB.

3. Force control

Since the proposed in-pipe robot in this paper is equipped with a manipulator, through which operational tasks are supposed to be undertaken, it is essential to neutralize the applied external forces from the environment to the end-effector of the robot, so that the robot can work efficiently. Therefore, it is required to employ a kind of force control and calculate the required torque of the motors in order to cancel the external forces applied on the end-effector using a Jacobian matrix.

The proposed controller in this paper is a classical impedance control which is combined with inverse dynamics in order to simultaneously control the position and force of the manipulator. This control is required for the operational tasks of the robot, in which both position and force should be set as a desired value. In this method, three torques should be calculated and implemented on the robot; the first torque is related to the inverse dynamics of the robot in order to provide the required torque of the joints to track the desired path τ_{dyn}, the second is the resistance torque corresponding to the resisting force implemented by the environment and the pipe wall on the end-effector, which should be neutralized in order to modify the desired path of the end-effector, τ_{res}, and the final one is the controlling torque which provides the feedback terms of error between the desired and actual position of the end-effector and is responsible for modifying the motion of the end-effector in a closed loop system using the feedback signals τ_{cont} [33]:

$$\tau_{tot} = \tau_{dyn} + \tau_{res} + \tau_{cont}. \tag{12}$$

The computed torque related to the inverse dynamics of the robots is calculated in Eq. (8). If the motion of the end-effector on the internal wall of the pipe is supposed as slippery, then the external force has a perpendicular component to the wall and two planar components in the tangential plane of the wall, and these components could be calculated with respect to each other. Considering Figure 1 and supposing that the applied force on the end-effector from the environment along the x coordinate is f with a friction coefficient of μ it can be shown easily that as a result of the frictional forces of the internal side of the pipe wall, we have the following external vector of force as the externally applied force on the end-effector:

$$F = -\begin{bmatrix} f \\ \mu f \frac{\dot{y}_3}{\sqrt{\dot{y}_3^2+\dot{z}_3^2}} \\ \mu f \frac{\dot{z}_3}{\sqrt{\dot{y}_3^2+\dot{z}_3^2}} \end{bmatrix}, \tag{13}$$

where f is the normal force between the end-effector and the internal wall of the pipe. Thus, considering the static equilibrium principal, the required torques of the motor to cancel the mentioned calculated external force can be provided as:

$$\tau_{res} = J^T F = -f \begin{bmatrix} \mu \frac{\dot{z}_3 C_{\beta_1+\beta_2} - a_2 \dot{y}_3 S_{\beta_1+\beta_2}}{\sqrt{\dot{y}_3^2+\dot{z}_3^2}} \\ \mu \frac{\dot{z}_3 S_{\beta_1+\beta_2} + a_2 \dot{y}_3 C_{\beta_1+\beta_2}}{\sqrt{\dot{y}_3^2+\dot{z}_3^2}} \\ r \end{bmatrix}. \tag{14}$$

It can be seen from the above equation that during the translational motion mode of the robot, when no operational task is being undertaken, the external force is $f = 0$, which results in zero torque for the motors, as expected. Finally, the closed loop controlling torques can be estimated based on a PD linear controller since it is supposed that using the first two feedforward controlling terms, the error of the end-effector is small enough to be compensated by a linear closed loop strategy:

$$\tau_{cont} = KJe + LJ\dot{e} = \begin{bmatrix} k_1 & 0 & 0 \\ 0 & k_2 & 0 \\ 0 & 0 & k_3 \end{bmatrix} J \begin{bmatrix} x_r - x_a \\ y_r - y_a \\ z_r - z_a \end{bmatrix} + \begin{bmatrix} l_1 & 0 & 0 \\ 0 & l_2 & 0 \\ 0 & 0 & l_3 \end{bmatrix} J \begin{bmatrix} \dot{x}_r - \dot{x}_a \\ \dot{y}_r - \dot{y}_a \\ \dot{z}_r - \dot{z}_a \end{bmatrix}, \tag{15}$$

where K and L are the controlling gains of the proportional and derivative error of the workspace and should be multiplied by the Jacobian matrix to provide the required torque of the joint space. The employed controlling strategy of this paper is impedance control, through which both position and force control will be implemented simultaneously. This strategy is used here to enable the robot to perform operational tasks within the pipe, such as welding, for which both tracking accuracy and force accuracy are necessary. Thus, to meet this goal, three components of the motors' torque need to be calculated and added together to be applied to the robot:

1. The CTM, through which the required feedforward torque of the motors is calculated using inverse dynamics to cover the desired trajectory tracking of the end-effector;
2. Force control, through which the required torques for neutralizing the external force of the end-effector are calculated as explained above;
3. Feedback control, through which the position and velocity error between the actual and desired position of the end-effector can be canceled as a result of kinematic and kinetic error sources such as compliance between the end-effector and the pipe wall.

Therefore, the required torque using impedance control can be calculated as follows:

$$\tau_{tot} = \tau_{dyn} + \tau_{res} + \tau_{cont} = \begin{bmatrix} \frac{1}{2} r^2 \ddot{\theta}(2m_{a_1} + 2m_{a_2} + 2m_b + 9m_w) + 3rF_S \\ \ddot{\beta}_2 \left(\frac{1}{3} m_{a_2} a_2^2 + \frac{1}{2} m_{a_1} r_{a_1}^2\right) + \frac{1}{2} m_{a_2} g a_2 C_{\beta_1+\beta_2} \\ \frac{1}{6} m_{a_2} \left(-2a_2 \dot{\beta}_2^2 + 6\ddot{a}_2 + 3gS_{\beta_1} + \beta_2\right) \end{bmatrix}$$

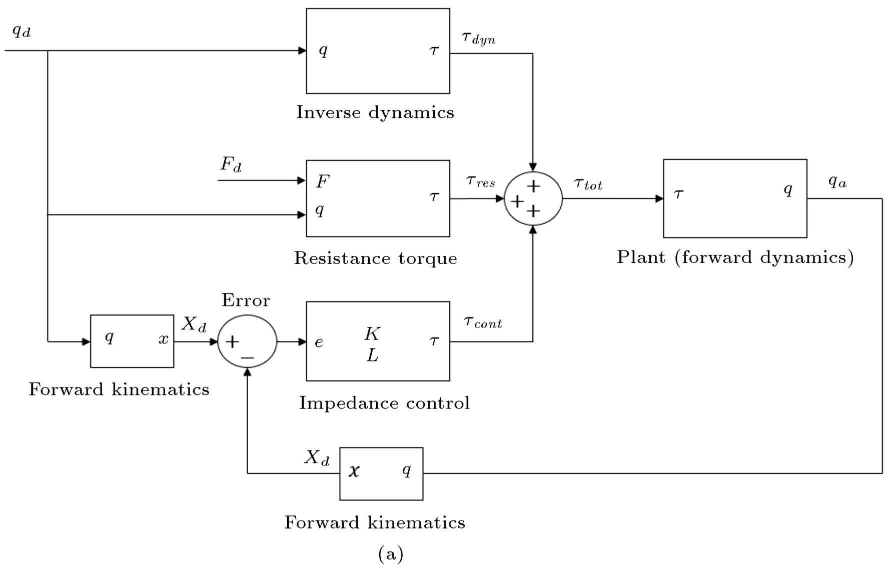

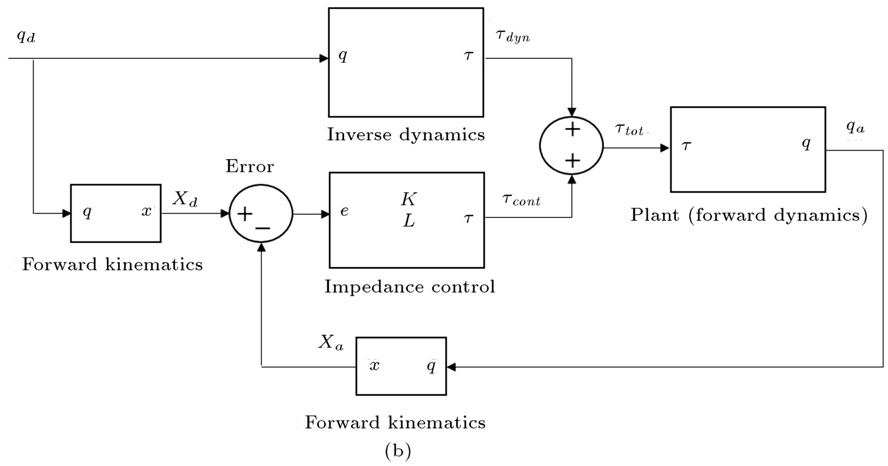

Figure 2. Overall scheme of the designed force controller compared with the ordinary Computed Torque Method (CTM).

$$
- f \begin{bmatrix} \mu \frac{\dot{z}_3 C_{\beta_1+\beta_2} - a_2 \dot{y}_3 S_{\beta_1+\beta_2}}{\sqrt{\dot{y}_3^2+\dot{z}_3^2}} \\ \mu \frac{\dot{z}_3 S_{\beta_1+\beta_2} + a_2 \dot{y}_3 C_{\beta_1+\beta_2}}{\sqrt{\dot{y}_3^2+\dot{z}_3^2}} \\ r \end{bmatrix}
+ \begin{bmatrix} k_1 & 0 & 0 \\ 0 & k_2 & 0 \\ 0 & 0 & k_3 \end{bmatrix} J \begin{bmatrix} x_r - x_a \\ y_r - y_a \\ z_r - z_a \end{bmatrix}
+ \begin{bmatrix} l_1 & 0 & 0 \\ 0 & l_2 & 0 \\ 0 & 0 & l_3 \end{bmatrix} \begin{bmatrix} \dot{x}_r - \dot{x}_a \\ \dot{y}_r - \dot{y}_a \\ \dot{z}_r - \dot{z}_a \end{bmatrix}, \tag{16}
$$

where k indicates the gains of position error, l shows the same parameter for velocity error and indexes r, a show the reference and the actual position of the end-effector Cartesian coordinates, respectively. The overall scheme of the flowchart of the designed force controller and its comparison with ordinary CTM can be seen in Figure 2.

As seen in the first case, in which the impedance force controller is employed, two additional terms are added to the final applied torque to the plant including the resistance force of the environment and the closed loop linear compensator of the end-effector error, while these two terms are ignored in the conventional CTM method.

4. Simulation study

In this section, the correctness and efficiency of the designed model and controller of the robot are verified by the aid of some analytic and comparative simulations which are conducted in MATLAB-SIMULINK.

4.1. Model simulation

The kinematics and kinetics of the proposed in-pipe mobile manipulator are investigated in this section

Table 3. Considered values of the engaged parameters of the designed robot.

Symbol	Explanation	Value	Unit
r	Wheels radius	0.4	m
ra_1	The radius of the first link	0.05	m
β_1	The initial angle of the robot	0	Rad
g	Gravitational acceleration	9.81	m/s^2
m_b	Mass of the robot chassis	0.5	kg
m_w	Mass of the wheels	0.1	kg
m_{a_1}	Mass of the first link	0.2	kg
m_{a_2}	Mass of the second link	0.2	kg
a_1	Length of the first link	0.2	m
F_s	Friction force of each wheel	1.16	N

considering the parameters of Table 3 and pipe radius of ($r = 0.2$ m). The desired path in the joint space of the robot is supposed as follows, which is a respiratory motion wherein the end effector reaches its initial position after 10 seconds:

$$q=\begin{bmatrix}\theta\\ \beta_2\\ a_2\end{bmatrix}=\begin{bmatrix}\frac{0.2\sin^3\left(\frac{\pi}{10}t\right)}{r}\\ 4\pi\sin\left(\frac{\pi}{20}t\right)\\ \frac{1}{3}\sin\left(\frac{\pi}{5}t\right)+0.4\end{bmatrix}. \tag{17}$$

The workspace movement of the robot end-effector is extracted as Figure 3.

It can be seen that the end-effector of the robot in which the tool is installed can move through any desired path within the internal surface of the pipe in a respiratory way. Also, the required generalized forces of the actuators can be extracted using the dynamic model of the system, as Figure 4.

It can be seen that the required motor torque related to the passive wheels of the robot are roughly constant during its motion along a unique direction. Its value changes when the robot is moving backwards which is expected according to the nature of the friction pipe. The torque and force of the motor and jack related to the manipulator are also changing in such a way that the desired path can be covered.

4.2. Model verification

The values given in Table 3 are considered for verification of the model in MATLAB.

In order to verify the model, two procedures are considered. Firstly, a path is considered and the desired and actual paths are compared for both of the kinematics and kinetics model. Afterwards, the response of the simulated model in MATLAB is compared with the profiles of the robot modeled and simulated in ADAMS. First, the extracted kinematic model of the robot is simulated, and its correctness is verified by comparing the inverse and direct input and output. The following path is considered as the desired trajectory of the end-effector workspace:

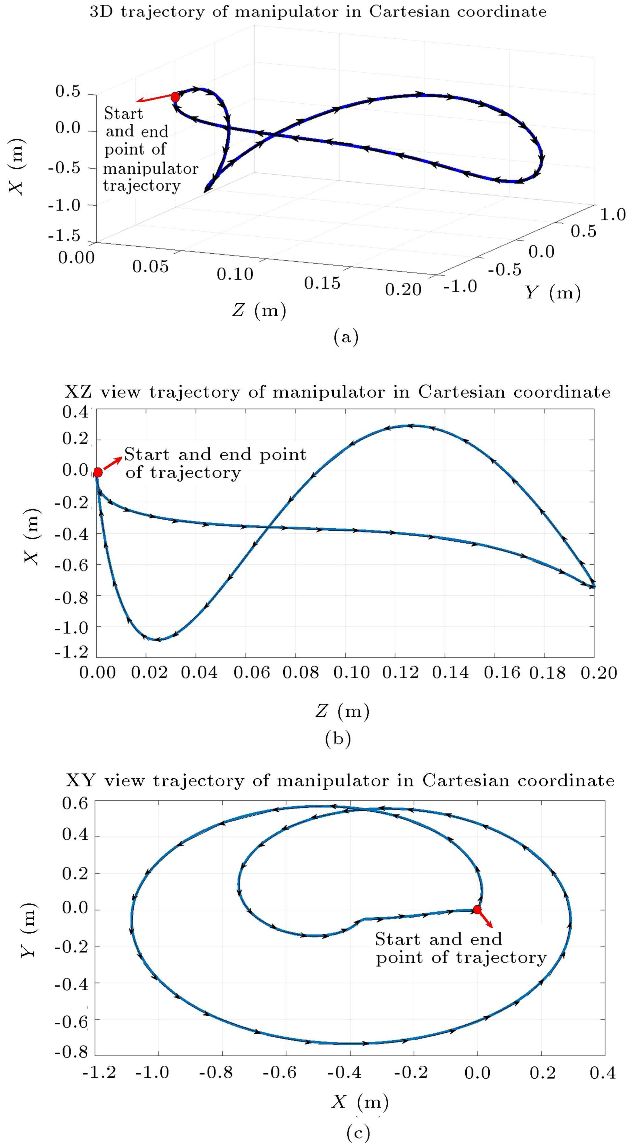

Figure 3. Actual tracked trajectory of the end-effector of the in-pipe robot.

$$\begin{bmatrix}x\\ y\\ z\end{bmatrix}=\begin{bmatrix}\frac{2t+0.1}{5t+3}\\ \sqrt{0.16-x^2}\\ 0.3\sin(0.3t)\end{bmatrix},\qquad |x|\le 0.4. \tag{18}$$

The actual workspace trajectory of the end-effector on the interior surface of the pipe wall is as Figure 5.

By solving the inverse kinematics of the robot, the joint space paths, according to the desired workspace, are extracted, as shown in Figure 6.

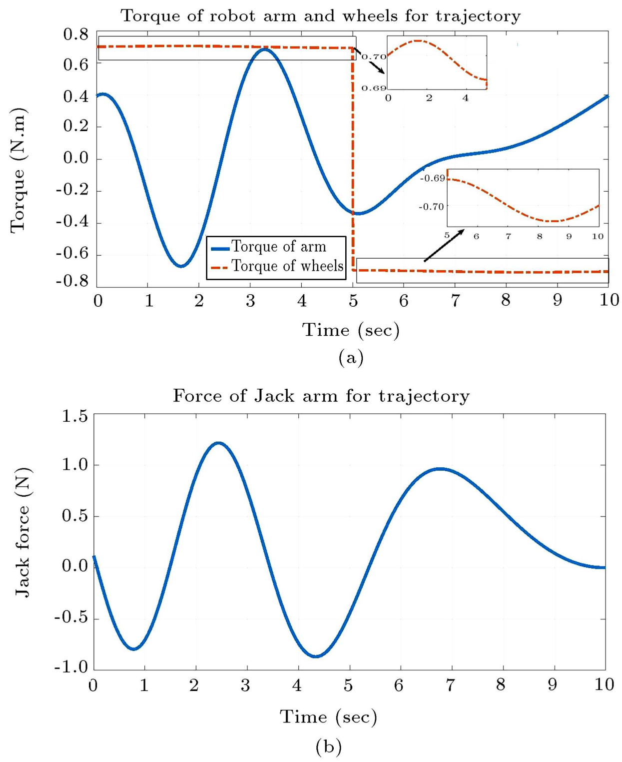

Figure 4. Required generalised forces of the robot actuators.

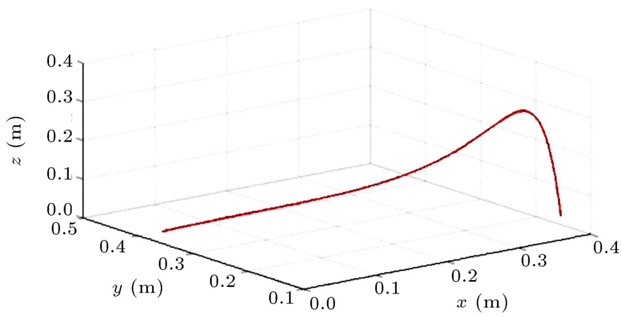

Figure 5. 3-D trajectory of the end-effector on the interior wall of the pipe.

Now, in order to verify the correctness of the modeling, the above result of joint space which is extracted using inverse kinematics is fed as the input of the forward kinematics and the relevant actual workspace of the end-effector is calculated as a function of time. Then, it is compared with the desired input of the robot workspace. As can be seen, the actual path of the end-effector has a good compatibility with the desired path, which is stated in Eq. (18) showing the correctness and accuracy of the kinematic modeling.

The same procedure is conducted in order to verify the extracted dynamic model of the robot. A desired path for the end-effector is considered as the input of inverse dynamics of the system, and the relevant required torques of the motors are calculated. Afterwards, the calculated torques are applied to the direct dynamics of the robot plant to check the actual movement of the end-effector and its compatibility with the desired one. Since the dynamic equation is extracted considering joint space as the generalized coordinates, the desired path is given in the joint space as:

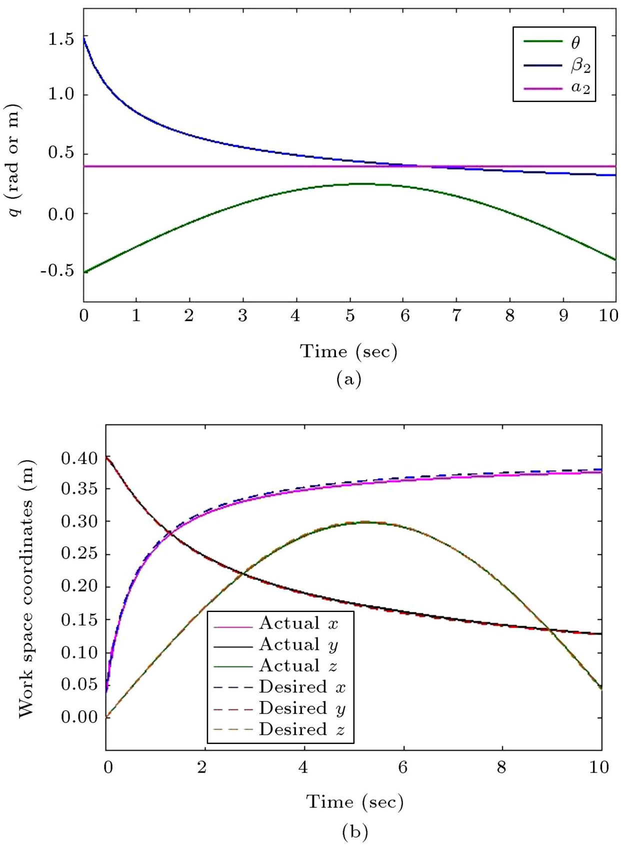

Figure 6. (a) Required joint space of the robot and (b) comparison of the actual and desired workspace of the robot.

$$q=\begin{bmatrix}\theta\\ \beta_2\\ a_2\end{bmatrix}=\begin{bmatrix}15\sin(0.1t)\\ 5\cos(t/15)\\ 0.4\end{bmatrix}. \tag{19}$$

Thus, the required motors' torque (and force) considering the extracted inverse dynamics of Eq. (9) and comparison of the actual and desired paths of the robot as a result of the implemented motors' torque can be seen in Figure 7.

Again, here, good compatibility can be observed between the actual and desired trajectories of the robot through which the correctness of dynamic modeling can be verified.

The correctness of the proposed model is also verified by modeling the robot in ADAMS and comparing its simulation results with the results of MATLAB. Considering the parameters of Table 3 with the pipe radius as ($r = 0.2$). Furthermore, suppose that the robot has to move through the desired trajectory of

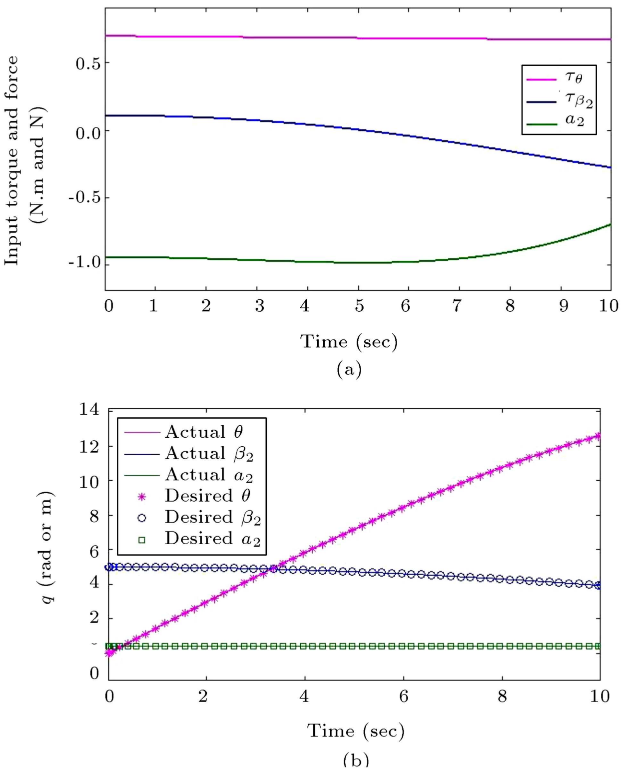

Figure 7. (a) Required motors' torque of the robot and (b) comparison of actual and desired path of the robot as a result of implemented motors' torque.

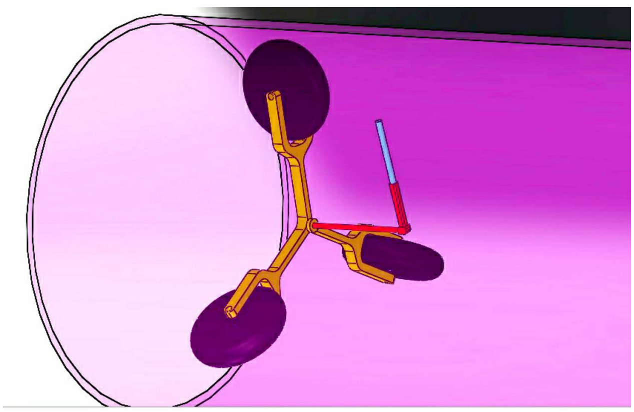

Figure 8. Scheme of the proposed in-pipe robot modelled in ADAMS.

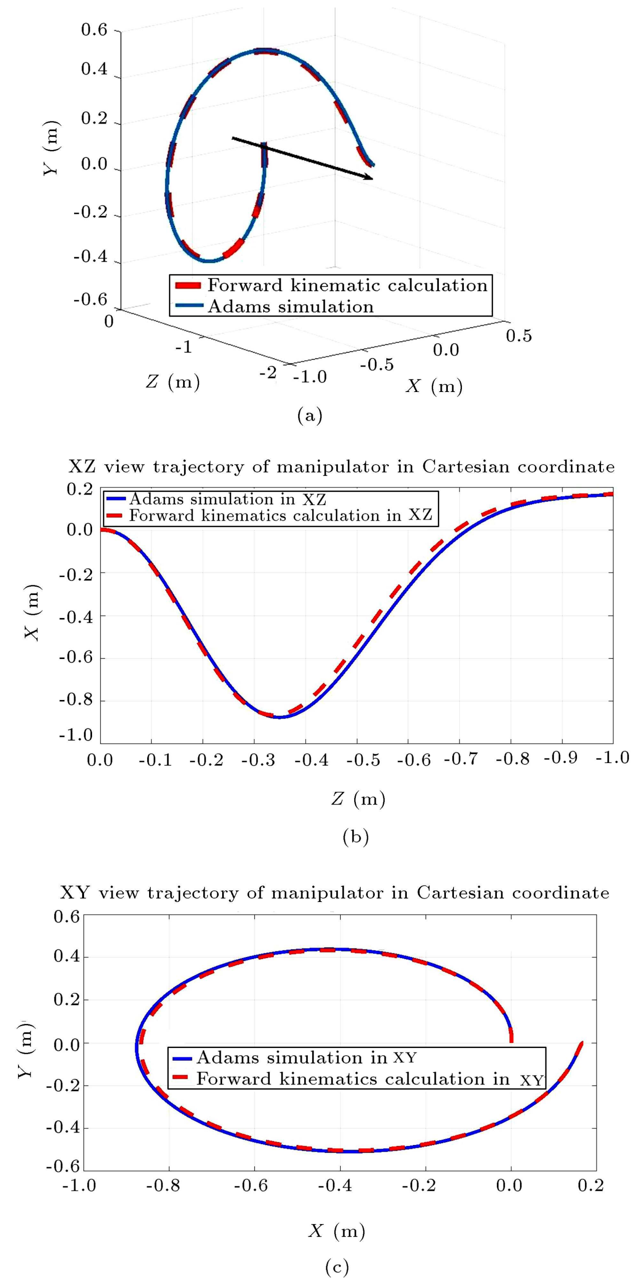

Figure 9. Trajectory in Cartesian coordinate compared with MSC ADAMS.

Eq. (20), in its joint space:

$$q = \begin{bmatrix} \theta \\ \beta_2 \\ a_2 \end{bmatrix} = \begin{bmatrix} \frac{-0.1t}{r} \\ 2\pi \sin\left(\frac{\pi}{20}t\right) \\ 0.2\sin\left(\frac{1}{10}t\right) + 0.4 \end{bmatrix}. \qquad (20)$$

A schematic view of the modeled system of the proposed in-pipe robot in ADAMS can be seen in Figure 8.

Comparison of the tracked trajectory between MATLAB and ADAMS in the workspace is shown in Figure 9. It can be seen that a good compatibility exists between the results of MATLAB and ADAMS with good accuracy, which shows the correctness of the modeling of the system.

As seen, the required force of the manipulator jack and also the torque of the motors are satisfactorily similar between MATLAB and ADAMS, which shows that the dynamic model is also correctly extracted. It can be seen that the required torque of the propulsion motor is roughly constant since the robot is moving without significant acceleration. Also, the vibrating response of the torque profile related to ADAMS has contributed to the stiffness characteristics of the

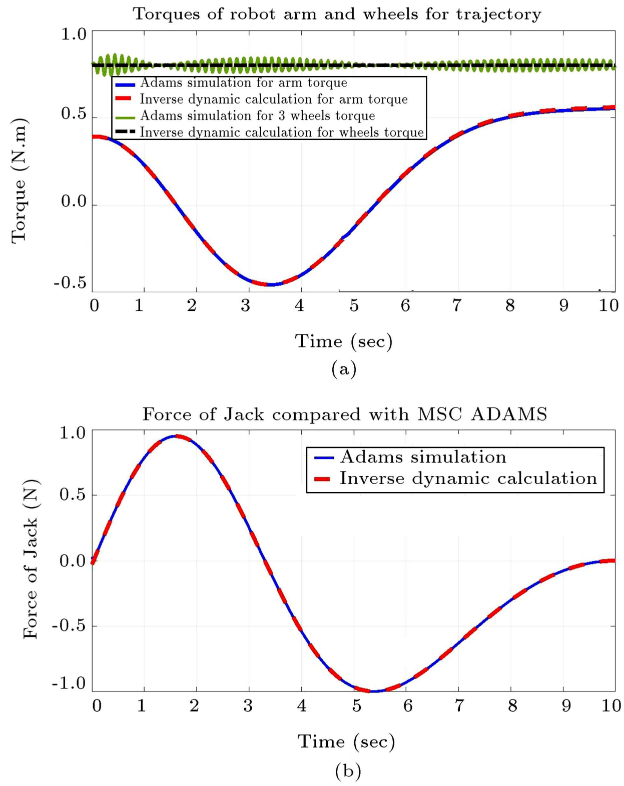

Figure 10. Comparison of the required generalized force between MATLAB and ADAMS.

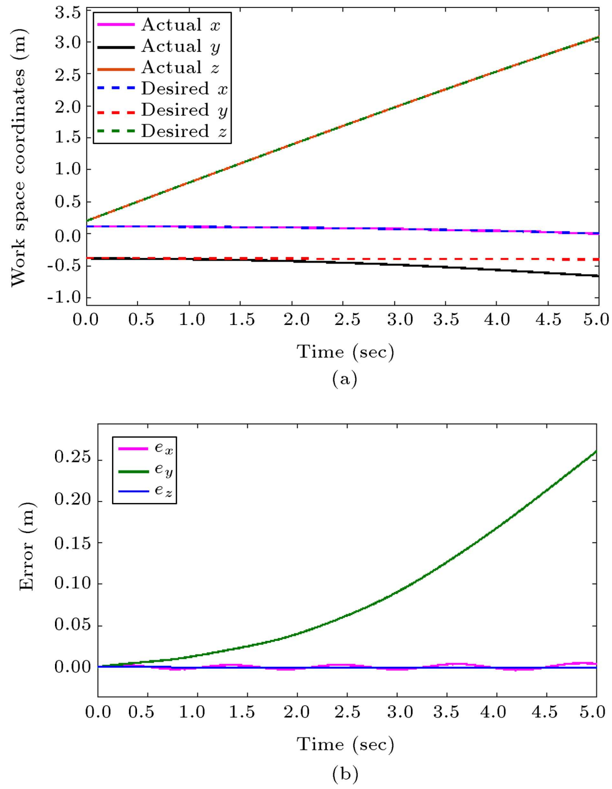

Figure 11. Comparison of the desired and actual path of the manipulator during manipulation while Computed Torque Method (CTM) controller is employed (a) and its resultant error (b).

surface contact between the passive wheels and the pipe surface, which is not modeled in MATLAB.

The corresponding comparison of the required generalized force also can be seen in Figure 10.

4.3. Verification of the designed impedance controller

In this section, a scenario and simulation is prepared in MATLAB, in order to verify the efficiency of the designed impedance controller. The robot and its manipulator is supposed to move within a predefined trajectory of Eq. (19), while a resisting force is implemented on its tool as a function of time inside the pipeline, for example as a result of a welding operation, and this force can be estimated using Eq. (13), considering the following parameters:

$$[f, \mu] = [2, 0.1]. \tag{21}$$

Also, the selected controlling gains of the position and velocity errors are considered as Eq. (22). Two simulations are conducted to check the efficiency of the designed force controller.

$$K = \begin{bmatrix} 1.5 & 0 & 0 \\ 0 & 0.5 & 0 \\ 0 & 0 & 0.5 \end{bmatrix}; \qquad L = \begin{bmatrix} 1 & 0 & 0 \\ 0 & 1 & 0 \\ 0 & 0 & 1 \end{bmatrix}. \tag{22}$$

For both cases, the mentioned external force of manipulation is applied on the plant. But, in the first case, a simple controller based on the CTM is employed to control the manipulation process, while, in the second, the mentioned designed force controller of Eq. (16) is applied. A disturbance is also implemented on the system based on the following function to examine the robustness of the designed controllers:

$$\tau^{(2)}_{man} = (0.2\sin(80t) + 1)\tau^{(1)}_{man}, \tag{23}$$

where $\tau^{(1)}_{man}$ is the computed torque for the manipulation process and $\tau^{(2)}_{man}$ is the summation of the computed torque together with disturbances. Considering the desired path of Eq. (19), the manipulator's actual path, wherein the system is controlled using the ordinary CTM, is depicted in Figure 11 with related error, while the above disturbance is being implemented on the robot.

It can be observed that as a result of the manipulation process, a deviation from the desired path is started and seems to be increasing as a result of the implemented manipulation force, which is not compensated for by a proper force controller. The actual and desired force profile and its corresponding errors are as Figure 12 for this case.

It can be seen that the desired and actual force

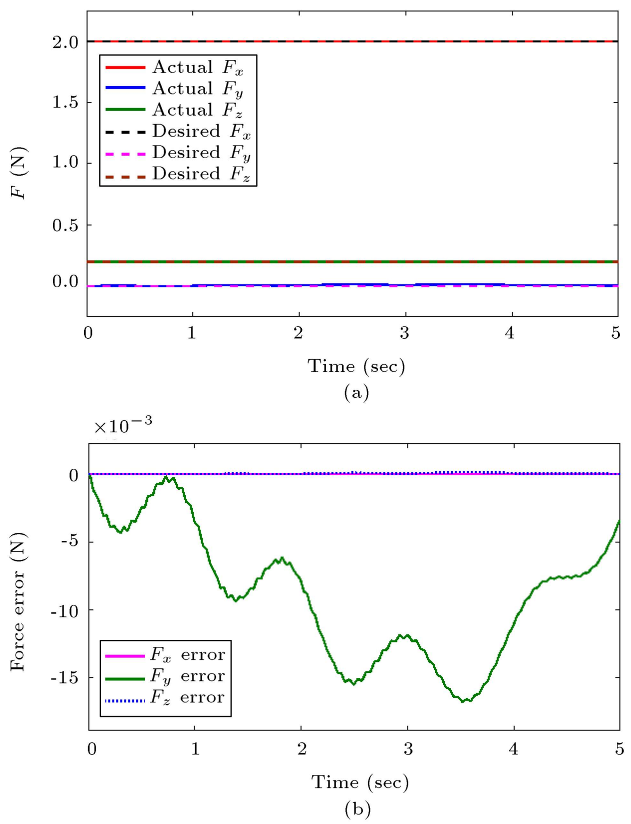

Figure 12. Comparison of the desired and actual force of the manipulator during manipulation while Computed Torque Method (CTM) controller is employed (a) and its resultant error (b).

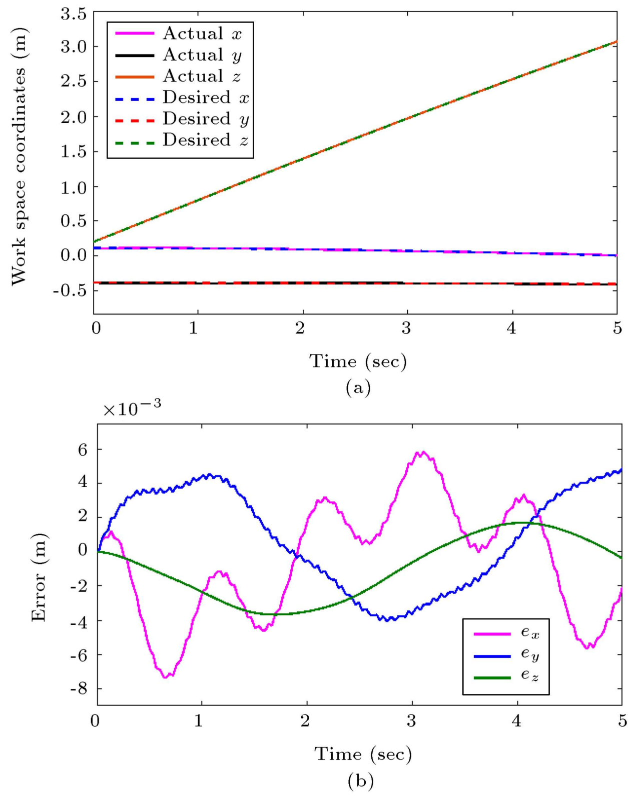

Figure 13. Comparison of the desired and actual path of the manipulator during manipulation while impedance control controller is employed (a) and its resultant error (b).

have an error of order 10^{-3}. Also, the required motors' torque, in this case, is as Figure 7.

However, for the case in which the force controller is employed, the above profiles of the manipulator path and its related error are modified as Figure 13. It can be seen that for the case in which the impedance control is designed and added to the robot controller, contrary to the CTM method, the actual path is compatible with the desired one with an error less than $6 * 10^{-3}$ m, while this error is over 0.2 m for the conventional CTM. The mentioned result proves that for a repairing robot, when an operational task is supposed to be covered, the design and implementation of a proper closed loop force control is necessary since the external forces need to be neutralized.

Corresponding implemented force on the manipulator tool and the related error between the actual and desired forces are as Figure 14.

Here again, the error is under 8×10^{-3}, which is the half of the force error related to the case of CTM with about 18×10^{-3}. Thus, using the proposed force control not only provides a good position control for the end-effector of the mobile manipulator but also results in good accuracy for the implemented force of the manipulator. The required motors' torque in this controlling method is as Figure 15. Here, the vibrating response of the motor contributes to compensating for the destructive effect of external disturbances.

It can be seen that the designed in-pipe robot equipped by the proposed impedance controller not only provides more accurate tracking but also provides the required tool force for the manipulation process during operational tasks.

5. Conclusion

In this paper, a new in pipe robot was designed, modeled and controlled, through which, not only could inspection of the pipelines be covered, but also manipulation, and the operational task can be conducted using the designed and installed manipulator on the robot. The correct robot was designed whose locomotion is based on wall-pressed wheels, and a 3DOF manipulator is mounted on the base of the robot so that the robot can move through the pipes and perform correctly. Kinematic and kinetic models of the whole robot, consisting of a mobile chassis and manipulator, were extracted in its forward and inverse phases. It was explained that since the robot is responsible for performing operational tasks, force control is extremely necessary as a design for the manipulator to provide the

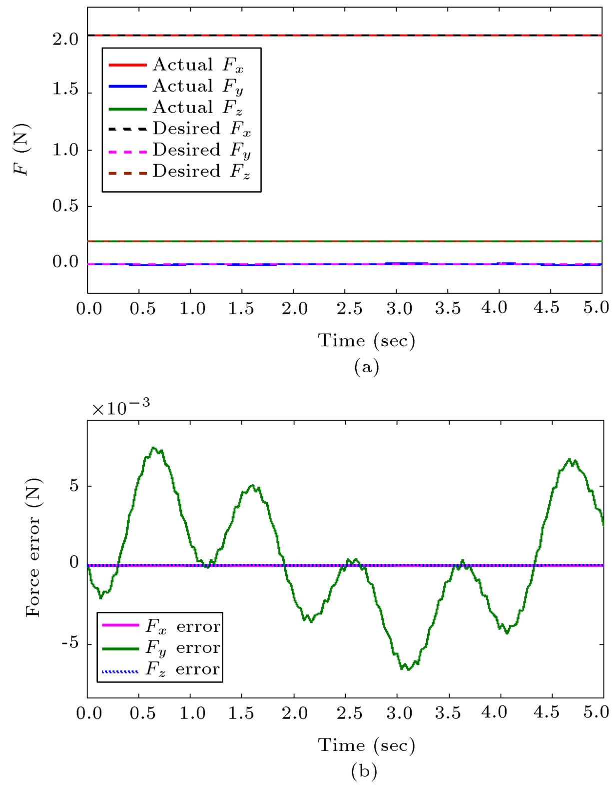

Figure 14. Comparison of the desired and actual force of the end-effector with impedance control (a) and its related error (b).

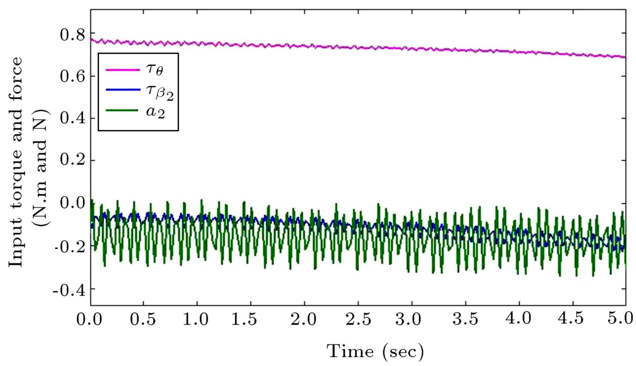

Figure 15. Motors' torque and force in impedance control.

sufficient operating force of the manipulation process. Thus, a controller was designed for the robot through which not only was its position controlled using the feedforward term of inverse dynamics, but also, its applied force is controllable using the designed impedance controller. The correctness of modeling and efficiency of the designed controller were verified afterwards using a different series of analytic and comparative simulation scenarios performed in MATLAB-SIMULINK. It was seen that the actual and desired path of the inverse and direct kinematics and kinetics are satisfactorily compatible, which proves the correctness of the modeling of the robot. The correctness of modeling was also verified by modeling the proposed robot in ADAMS and comparing the related kinematics and kinetic results with MATLAB. The good compatibility of the results showed the correctness of modeling. Finally, the efficiency of the designed controller was proved through a scenario, in which the robot is performing an operational task, and some external forces are applied to the end-effector. It was shown that the robot, which is equipped with a simple feedforward term of controlling, fails to move within the desired path. Implementation of the correct force on the robot, which is equipped by the proposed impedance control, showed that it could handle both the desired position and the required implemented force simultaneously. The error of the ordinary controller was of order 10^{-1} m while this deviation is compensated in the proposed controller to 10^{-3} m. The same result was also obtained for the accuracy of the implemented force, which was improved about two times (decrease from 16×10^{-3} to 8×10^{-3}) in the proposed force control case. Also, it was seen that the required motor torque related to the proposed impedance controller has a vibrating response compared to a simple Computed Torque Method (CTM). This vibrating torque is required to neutralize the destructive effect of oscillatory disturbance implemented on the robot. Therefore, this paper shows that the proposed in-pipe robot equipped by the manipulator and impedance controller can move through the pipeline installations and cover both inspectional and operational tasks successfully.

References

1. Thanjavur, K. and Rajagopalan, R. "Ease of dynamic modelling of Wheeled Mobile Robots (WMRs) using Kane's approach", In *Proceedings of International Conference on Robotics and Automation, IEEE* (1997).
2. Tanner, H.G. and Kyriakopoulos, K.J. "Mobile manipulator modeling with Kane's approach", *Robotica*, **19**(6), pp. 675–690 (2001).
3. Korayem, M. and Shafei, A. "A new approach for dynamic modeling of n-viscoelastic-link robotic manipulators mounted on a mobile base", *Nonlinear Dynamics*, **79**(4), pp. 2767–2786 (2015).
4. Korayem, M. and Dehkordi, S. "Derivation of motion equation for mobile manipulator with viscoelastic links and revolute-prismatic flexible joints via recursive Gibbs-Appell formulations", *Robotics and Autonomous Systems*, **103**, pp. 175–198 (2018).
5. Korayem, M., Shafei, A., and Shafei, H. "Dynamic modeling of nonholonomic wheeled mobile manipulators with elastic joints using recursive Gibbs-Appell formulation", *Scientia Iranica*, **19**(4), pp. 1092–1104 (2012).
6. Korayem, M., Yousefzadeh, M., and Susany, S. "Dynamic modeling and feedback linearization control of

wheeled mobile cable-driven parallel robot considering cable sag", *Arabian Journal for Science and Engineering*, **42**(11), pp. 4779–4788 (2017).

7. Korayem, M. and Shafei, A. "Motion equation of nonholonomic wheeled mobile robotic manipulator with revolute-prismatic joints using recursive Gibbs-Appell formulation", *Applied Mathematical Modelling*, **39**(5–6), pp. 1701–1716 (2015).

8. Emami, M., Zohoor, H., and Sohrabpour, S. "Solving high order nonholonomic systems using Gibbs-Appell method", in *BSG Proceedings* (2009).

9. Roslin, N.S., Anuar, A., Jalal, M.F.A., et al. "A review: Hybrid locomotion of in-pipe inspection robot", *Procedia Engineering*, **41**, pp. 1456–1462 (2012).

10. Fukuda, T., Hosokai, H., and Uemura, M. "Rubber gas actuator driven by hydrogen storage alloy for in-pipe inspection mobile robot with flexible structure", In *Proceedings, 1989 International Conference on Robotics and Automation, IEEE* (1989).

11. Roman, H.T., Pellegrino, B., and Sigrist, W. "Pipe crawling inspection robots: an overview", *IEEE Transactions on Energy Conversion*, **8**(3), pp. 576–583 (1993).

12. Iwashina, S., Hayashi, I., Iwatsuki, N., et al. "Development of in-pipe operation micro robots", In *1994 5th International Symposium on Micro Machine and Human Science Proceedings, IEEE* (1994).

13. Li, P., Yang, W., Jiang, X., et al. "Active screw-driven in-pipe robot for inspection", In *2017 IEEE International Conference on Unmanned Systems (ICUS), IEEE* (2017).

14. Ciszewski, M., Buratowski, T., and Giergiel, M. "Modeling, simulation and control of a pipe inspection mobile robot with an active adaptation system", *IFAC-PapersOnLine*, **51**(22), pp. 132–137 (2018).

15. Nayak, A. and Pradhan, S. "Design of a new in-pipe inspection robot", *Procedia Engineering*, **97**, pp. 2081–2091 (2014).

16. Chang, F.-S., Hwang, L.-T., Liu, C.-F., et al. "Design of a pipeline inspection robot with belt driven ridged cone shaped skate model", In *2015 IEEE International Conference on Robotics and Biomimetics (ROBIO), IEEE* (2015).

17. Ciszewski, M., Mitka, L., Buratowski, T., et al. "Modeling and simulation of a tracked mobile inspection robot in MATLAB and V-REP software", *Journal of Automation Mobile Robotics and Intelligent Systems*, **11**(2), pp. 5–11 (2017).

18. Gargade, A.A. and Ohol, S.S. "Development of actively steerable in-pipe inspection robot for various sizes", In *Proceedings of the Advances in Robotics, ACM* (2017).

19. Ibrahimov, B. "Development of a decision making guide for locomotion design for in-pipe inspection robots-one step towards open innovation in robotics", *IFAC-PapersOnLine*, **49**(29), pp. 77–82 (2016).

20. Kwon, Y.-S. and Yi. B.-J. "The kinematic modeling and optimal paramerization of an omni-directional pipeline robot", In *2009 IEEE International Conference on Robotics and Automation, IEEE* (2009).

21. Chablat, D., Venkateswaran, S., and Boyer, F. "Mechanical design optimization of a piping inspection robot", In *28th CIRP Design Conference* (2018).

22. Gravalos, I., Loutridis, S., Gialamas, T., et al. "Dynamic behaviour of an in-pipe sensor-based platform for soil water monitoring", *Computers and Electronics in Agriculture*, **134**, pp. 11–18 (2017).

23. Zhang, Y. and Yan, G. "In-pipe inspection robot with active pipe-diameter adaptability and automatic tractive force adjusting", *Mechanism and Machine Theory*, **42**(12), pp. 1618–1631 (2007).

24. Kwon, Y.-S., Lim, H., Jung, E.-J., et al. "Design and motion planning of a two-moduled indoor pipeline inspection robot", In *2008 IEEE International Conference on Robotics and Automation, IEEE* (2008).

25. Zhang, X. and Chen, H. "Independent wheel drive and fuzzy control of mobile pipeline robot with vision", In *IECON'03. 29th Annual Conference of the IEEE Industrial Electronics Society (IEEE Cat. No. 03CH37468), IEEE* (2003).

26. Gregory, J., Olivares, A., and Staffetti, E. "Energy-optimal trajectory planning for robot manipulators with holonomic constraints", *Systems & Control Letters*, **61**(2), pp. 279–291 (2012).

27. Li, Z., Yang, C., and Gu, J. "Neuro-adaptive compliant force/motion control of uncertain constrained wheeled mobile manipulators", *International Journal of Robotics and Automation*, **22**(3), pp. 206–214 (2007).

28. Carelli, R. and Kelly, R. "An adaptive impedance/force controller for robot manipulators", *IEEE Transactions on Automatic Control*, **36**(8), pp. 967–971 (1991).

29. Parra-Vega, V. and Arimoto, S. "A passivity-based adaptive sliding mode position-force control for robot manipulators", *International Journal of Adaptive Control and Signal Processing*, **10**(4–5), pp. 365–377 (1996).

30. Doulgeri, Z. and Arimoto, S. "A position/force control for a robot finger with soft tip and uncertain kinematics", *Journal of Robotic Systems*, **19**(3), pp. 115–131 (2002).

31. Cheah, C.-C., Kawamura, S., and Arimoto, S. "Stability of hybrid position and force control for robotic manipulator with kinematics and dynamics uncertainties", *Automatica*, **39**(5), pp. 847–855 (2003).

32. Spong, M.W., Hutchinson, S., and Vidyasagar, M., *Robot Modeling and Control*, John Wiley & Sons, Inc. (2006).

33. Villani, L. and De Schutter, J., *Force Control*, In *Springer Handbook of Robotics*, Springer, pp. 195–220 (2016).

Biographies

Hami Tourajizadeh was born in Tehran, Iran on October 30, 1984. He received his PhD from IUST in the field of Mechanics (branch of control and robotics). The results of his research include more than 35 journal papers, 15 conference papers, 1 published book, 1 book chapter and 2 booked inventions. He has been involved in teaching and research activities for more than 10 years in different universities and has been Assistant Professor at Kharazmi University since 2013. His research interests include Robotics, Automotive Engineering, Control and Optimization.

Vahid Boomeri was born in Tehran, Iran, on January 24, 1989. He received his BS in Mechanical Engineering from the University of Semnan in 2015 and is now a MS graduate of Kharazmi University in the field of Applied Mechanical Design. One scientific research paper and two conference papers in the field of climbing robots are the results of his academic research so far. His research interests include, Parallel Robots, Mechanism Design, Adaptive and Robust Control and Manufacturing Robots.

Samira Afshari was born in Tehran, Iran on March 18, 1993. She is now an MS. student of Kharazmi University in the field of Applied Mechanical Design. One accepted journal paper is the result of her research activities so far. Her research interests include Robotic Systems and Control Methods.

Meisam Azimi was born in Bojnourd, Iran, on March 25, 1992. He is currently a MS graduate of Kharazmi University in the field of Applied Mechanical Design. His research interests include Robotic Systems, Modelling and Control Methods.